

Quasiparticle tunneling in a periodically driven bosonic Josephson junction

Bettina Gertjerenken* and Martin Holthaus

Institut für Physik, Carl von Ossietzky Universität, D-26111 Oldenburg, Germany

(Received 23 September 2014; published 19 November 2014)

A resonantly driven bosonic Josephson junction supports stable collective excitations, or quasiparticles, which constitute analogs of the Trojan wave packets previously explored with Rydberg atoms in strong microwave fields. We predict a quantum beating effect between such symmetry-related many-body Trojan states taking place on time scales which are long in comparison with the driving period. Within a mean-field approximation, this quantum beating can be regarded as a manifestation of dynamical tunneling. On the full N -particle level, the beating phenomenon leads to an experimentally feasible, robust strategy for probing highly entangled mesoscopic states.

DOI: [10.1103/PhysRevA.90.053622](https://doi.org/10.1103/PhysRevA.90.053622)

PACS number(s): 03.75.Lm, 03.75.Gg, 05.45.Mt, 67.85.-d

I. INTRODUCTION

The mechanism which effectuates the stability of ion motion in a Paul trap [1] also underlies the stability of the motion of the Trojan asteroids, which orbit around the Sun near stable Lagrange points of the Sun-Jupiter system. This stable celestial motion has a quantum-mechanical counterpart, discovered in 1994 by Bialynicki-Birula, Kaliński, and Eberly: If one exposes Rydberg electrons to strong microwave radiation, such that the classical Kepler frequency of the orbiting electron equals the frequency of the external driving electric microwave field, one finds stable, though nonstationary, quantum states which are described by nonspreading wave packets centered around a classical periodic orbit [2,3]. Such Trojan states were first realized with lithium Rydberg atoms in a linearly polarized microwave field [4] and still are the subject of ongoing research in atomic physics [5]. More generally, “Trojan” single-particle wave packets belong to Floquet states which are semiclassically attached to a nonlinear resonance island of the corresponding classical phase space, thus explaining their nondispersing nature [6,7].

It has been pointed out recently that Trojan states can also occur in periodically driven many-body systems, where they correspond to stable collective excitations, or quasiparticles, moving in phase with the driving force [8]. Here we show that there exists a genuinely quantum-mechanical beating effect between similar many-body Trojan states which perform *subharmonic* motion with respect to the drive; this beating can be understood as quasiparticle tunneling. In particular, we consider a resonantly driven bosonic Josephson junction, as provided by ultracold atoms in an optically generated double-well potential [9,10], or by the internal Josephson effect in a spinor Bose-Einstein condensate [11], and demonstrate that there is a quantum beating phenomenon between classically equivalent, Trojan-like collective subharmonic many-particle motions. Against the background of a mean-field approach this beating may be interpreted as dynamical tunneling in the sense of Davis and Heller, i.e., as quantum-mechanical tunneling between symmetry-related regular regions of classical phase space in the absence of a potential barrier [12,13]. However, the very core of this beating effect reveals itself on the

full N -particle quantum level, taking recourse neither to the mean-field picture nor to the entailing classical phase space, and suggests an interesting experimental option for creating and probing mesoscopic Schrödinger cat-like states. To lay out our reasoning we first sketch the basic mechanism in a quite general but approximate form in Sec. II, shifting technical details of the analysis to the Appendix. We then verify our deductions with the help of exact numerical model calculations in Sec. III, whereupon some remarks concerning possible experimental observations are made in Sec. IV.

II. THE BASIC TUNNELING SCHEME

We start by considering a quantum-mechanical nonlinear oscillator which may be given by either a single-particle or a many-particle system, formally described by a Hamiltonian H_0 with discrete energy eigenvalues E_n and eigenstates $|n\rangle$, so that $H_0|n\rangle = E_n|n\rangle$. We assume that the eigenvalues are ordered with respect to magnitude and vary smoothly with n around some particular state r , so that it is meaningful to take the formal derivative

$$\tilde{\omega}_r = \left. \frac{1}{\hbar} \frac{dE_n}{dn} \right|_{n=r}; \quad (1)$$

the frequency $\tilde{\omega}_r$ defined in this manner is the oscillation frequency of a wave packet mainly consisting of states in the vicinity of $n = r$. We further assume that this oscillator is exposed to an external influence described by some sinusoidally modulated operator V , such that the full Hamiltonian takes the form

$$H(t) = H_0 + \lambda V \cos(\omega t); \quad (2)$$

here λ is a dimensionless coupling strength. The key point now is that the driving frequency be chosen such that $\tilde{\omega}_r = \omega/\nu$, meaning that one oscillation cycle of the unperturbed system governed by H_0 is as long as ν cycles of the external drive, so that we have a $\nu:1$ resonance. The case $\nu = 1$ applies to the usual Trojans [3,7,8]; here we demand instead that $\nu \geq 2$ be a small integer larger than unity. It is then natural to search for solutions to the time-dependent Schrödinger equation of the form

$$|\Psi(t)\rangle = \sum_n c_n(t) |n\rangle \exp\left[-\frac{i}{\hbar} \left(E_r + (n-r) \frac{\hbar\omega}{\nu}\right) t\right], \quad (3)$$

*Present address: Department of Mathematics and Statistics, University of Massachusetts, Amherst, MA 01003-4515, USA.

where the sum again extends over states close to the resonant state $n = r$. Because of the resonance condition, the exponential exhibits the first-order expansions of the energies E_n around $n = r$. This implies that the remaining time dependence of the coefficients $c_n(t)$, given by the exact system

$$i\hbar\dot{c}_n(t) = \left(E_n - E_r - (n-r)\frac{\hbar\omega}{\nu}\right)c_n(t) + \lambda \cos(\omega t) \sum_m e^{i(n-m)\omega t/\nu} \langle n|V|m\rangle c_m(t), \quad (4)$$

should be relatively weak. Next, we employ three standard approximations [14,15]: We expand the energy eigenvalues up to second order according to

$$E_n \approx E_r + (n-r)\frac{\hbar\omega}{\nu} + \frac{1}{2}(n-r)^2 E_r'', \quad (5)$$

replace all matrix elements $\langle n|V|n \pm \nu\rangle$ by a representative constant v , and keep, in the spirit of the rotating-wave approximation, only the secular terms $m = n \pm \nu$, thus being led to the strongly simplified system

$$i\hbar\dot{c}_n = \frac{1}{2}(n-r)^2 E_r'' c_n + \frac{\lambda v}{2} (c_{n+\nu} + c_{n-\nu}). \quad (6)$$

This set of equations contains the essential physics of beating Trojans. As illustrated in Fig. 1 for the case $\nu = 2$, each coefficient c_n is coupled only to its remote neighbors $c_{n \pm \nu}$, resulting in ν separate subsets of coefficients. The mathematical analysis, carried through in detail in the Appendix, shows that

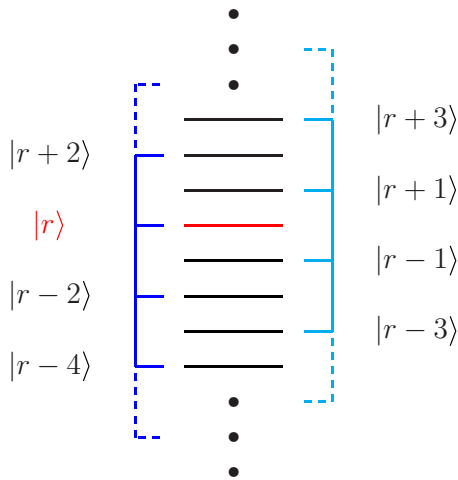


FIG. 1. (Color online) Principle of Trojan beating for $\nu = 2$: The unperturbed energy eigenstates $|n\rangle$ of a weakly anharmonic oscillator, with energy levels spaced by about $\hbar\omega/2$ in the vicinity of $n = r$ as indicated by the horizontal lines, are subjected to an external monochromatic perturbation with frequency ω . Resonant coupling then occurs between next-to-nearest neighbors, as expressed by Eq. (6), giving rise to two almost uncoupled “ladders” of states indicated by the vertical braces. Each ladder corresponds to a set of $2\pi/\omega$ -periodic Floquet states enumerated by a new quantum number k . Odd and even superpositions of the Floquet states with $k = 0$ yield two $4\pi/\omega$ -periodic Trojans, which beat among themselves on much longer time scales.

this Eq. (6) is the Fourier representation of a Mathieu equation, which formally equals the stationary Schrödinger equation of a fictitious quantum particle moving on a one-dimensional cosine lattice, with periodic Born–von Kármán boundary conditions imposed after ν potential wells [16]. This yields Bloch bands of energy eigenstates, labeled by the band index $k = 0, 1, 2, \dots$, each band containing ν states. Transformed back to the nonlinear oscillator considered here, these Bloch states provide solutions of the form

$$|\Psi_k^{(j)}(t)\rangle = e^{-i\eta_k^{(j)}t/\hbar} \sum_{\ell} f_{\ell,k}^{(j)} |r + j + \ell\nu\rangle \times \exp\left[-\frac{i}{\hbar}(E_r + j\hbar\omega/\nu + \ell\hbar\omega)t\right], \quad (7)$$

with $j = 0, 1, \dots, \nu - 1$ enumerating the states in the k th Bloch band, $f_{\ell,k}^{(j)}$ denoting the ℓ th Fourier coefficient of a Mathieu function specified in the Appendix, and $\eta_k^{(j)}$ being proportional to the energy of the Bloch state labeled by k and j , thus falling within the k th energy band.

Importantly, these approximate solutions conform to the Floquet theorem: Because the Hamiltonian (2) is periodic in time, $H(t) = H(t + T)$ with $T = 2\pi/\omega$, it gives rise to a complete set of Floquet states, that is, of *exact* solutions to the time-dependent Schrödinger equation which possess the particular form [17–19]

$$|\Psi_n(t)\rangle = |u_n(t)\rangle \exp(-i\varepsilon_n t/\hbar) \quad (8)$$

with $|u_n(t)\rangle = |u_n(t + T)\rangle$, and thus reproduce themselves perpetually in time, except for a phase factor determined by their respective quasienergy ε_n . Evidently, the above wave functions (7) are Floquet states with quasienergies

$$\varepsilon_k^{(j)} = E_r + j\hbar\omega/\nu + \eta_k^{(j)} \pmod{\hbar\omega}. \quad (9)$$

Hence, within the regime of validity of the above approximations a $\nu:1$ resonance leads to a characteristic ordering of the quasienergy spectrum of a driven nonlinear quantum oscillator, featuring ν sets of Floquet states with quasienergies displaced against each other by $\hbar\omega/\nu$. It is assumed here that the depth of the effective cosine lattice, which is proportional to the driving strength λ , is so large that there are several “below-barrier” bands. The Floquet states associated with the ground-state band $k = 0$ then are of particular interest: For $\nu = 1$, for which there is $j = 0$ only, the Floquet ground state $k = 0$ provides the archetypal Trojan, that is, the maximally localized nonspreading wave packet closely following the stable T -periodic orbit associated with a 1:1 resonance in classical phase space [7,8,15]; the states with $k \geq 1$ constitute its excitations.

The next link in the chain of reasoning again is suggested by the solid-state picture of a quasiparticle moving on a one-dimensional cosine lattice: From the extended Bloch waves pertaining to the same energy band of such a lattice one can construct Wannier functions which no longer are stationary energy eigenstates, but which are localized in the individual potential wells [16]. Analogously one may construct, for

instance, the linear combination

$$|\tilde{\Psi}_k(t)\rangle = \frac{1}{\sqrt{\nu}} \sum_{j=0}^{\nu-1} |\Psi_k^{(j)}(t)\rangle. \quad (10)$$

If all the $\eta_k^{(j)}$ were identical for $j = 0, \dots, \nu - 1$ (that is, if the k th Bloch band had a vanishing width), this state would correspond precisely to the k th excitation of a usual Trojan, but now with frequency ω/ν . Hence, it would remain perpetually localized around one of the ν equivalent classical νT -periodic orbits generated by a $\nu:1$ resonance according to the Poincaré-Birkhoff theorem [20], performing coherent motion which is subharmonic with respect to the driving frequency. However, quantum tunneling between the individual lattice wells bestows a finite width upon the bands, leading to slightly different $\eta_k^{(j)}$ and thus to a beating effect between ν Trojan-like wave packets, each following one of these ν orbits.

III. MODEL CALCULATIONS

We now apply these considerations to a specific many-body system: The unperturbed oscillator is given by the Lipkin-Meshkov-Glick Hamiltonian [21]

$$H_0 = -\frac{\hbar\Omega}{2}(a_1^\dagger a_2^\dagger + a_1^\dagger a_2) + \hbar\kappa(a_1^\dagger a_1^\dagger a_1 a_1 + a_2^\dagger a_2^\dagger a_2 a_2) + \hbar\mu_0(a_1^\dagger a_1 - a_2^\dagger a_2), \quad (11)$$

which describes a Bose-Einstein condensate in a tilted double-well potential [22,23]. Here the operators $a_j^{(\dagger)}$ annihilate (create) a Bose particle in well j ($j = 1, 2$), $\hbar\Omega$ is the single-particle tunneling splitting, $2\hbar\kappa$ denotes the repulsion energy of a pair of bosons occupying the same well, and $2\hbar\mu_0$ is the energetic misalignment of the two wells. We subject this bosonic Josephson junction (11) to an additional time-periodic tilt with amplitude $\hbar\mu_1$, such that the total Hamiltonian reads [24]

$$H(t) = H_0 + \hbar\mu_1 \sin(\omega t)(a_1^\dagger a_1 - a_2^\dagger a_2). \quad (12)$$

In Fig. 2 we plot the exact, numerically computed quasienergies of this system for $N = 200$ particles, scaled interaction strength $N\kappa/\Omega = 0.95$, scaled driving frequency $\omega/\Omega = 3.258$, and scaled tilt $\mu_0/\Omega = 0.5$ vs the scaled driving strength $2\mu_1/\omega$. Here $r = 142$ is a resonant level with $\nu = 2$, leading in accordance with Eq. (9) to two almost identical sets of quasienergies displaced against each other by $\hbar\omega/2$. As shown in the Appendix, the Mathieu theory yields a quite good description of these quasienergies, notwithstanding the somewhat crude approximations made, so that the analysis sketched in the previous section provides a sound basis for our deductions.

Next, we take the numerically computed exact superpositions

$$|\tilde{\Psi}_0^{(\pm)}(0)\rangle = (|\Psi_0^{(0)}(0)\rangle \pm |\Psi_0^{(1)}(0)\rangle)/\sqrt{2} \quad (13)$$

and follow their time evolution by solving the time-dependent N -particle Schrödinger equation: These states correspond to stable, Trojan-like collective many-particle excitations which have been termed “floton” quasiparticles in Ref. [8]; they should beat among themselves on a time scale determined

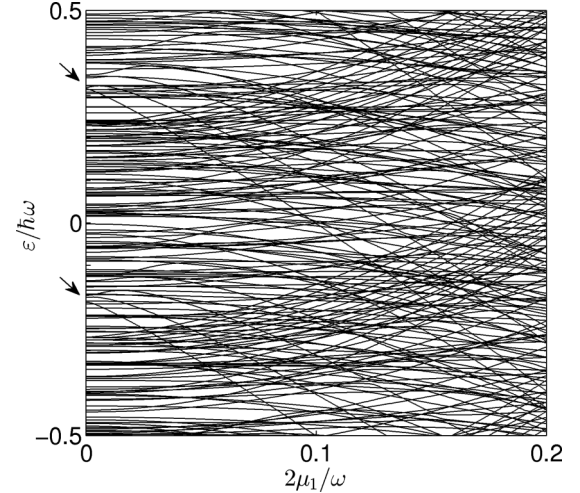


FIG. 2. Quasienergy spectrum of the tilted, driven bosonic Josephson junction (12) for $N = 200$ particles, $N\kappa/\Omega = 0.95$, $\omega/\Omega = 3.258$, and $\mu_0/\Omega = 0.5$. Under these conditions $r = 142$ is a resonant level with $\nu = 2$, leading to two almost identical sets of quasienergies displaced against each other by $\hbar\omega/2$, as predicted by the Mathieu theory. The Trojan doublet with $k = 0$ is indicated by the arrows.

by the tiny difference between the energies $\eta_0^{(0)}$ and $\eta_0^{(1)}$. Figure 3 shows results of such calculations, for both short and long times. Here we plot the experimentally measurable population difference $2\langle J_z \rangle/N$ between both wells, with $J_z = (a_1^\dagger a_1 - a_2^\dagger a_2)/2$. We first take $N = 100$ particles and fix the driving amplitude at the small value $2\mu_1/\omega = 0.025$,

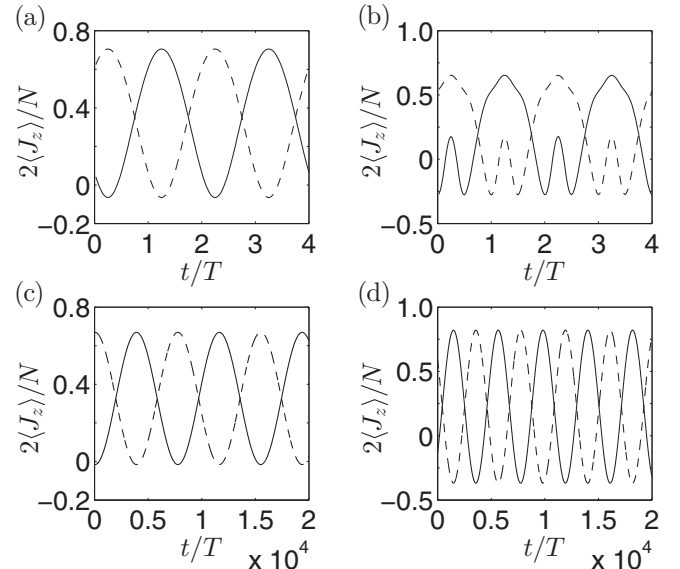


FIG. 3. Scaled population imbalance $2\langle J_z \rangle/N$ evolving from the Trojan initial states $|\tilde{\Psi}_0^{(+)}\rangle$ (solid lines) and $|\tilde{\Psi}_0^{(-)}\rangle$ (dashed lines). While the short-time evolution is monitored continuously, the long-time evolution is recorded stroboscopically at each multiple of $2T$. (a, c) $N = 100$, $2\mu_1/\omega = 0.025$; the other parameters are as in Fig. 2. (b, d) $N = 50$, $2\mu_1/\omega = 1.0$, $N\kappa/\Omega = 0.95$, $\omega/\Omega = 1.6$, and $\mu_0/\Omega = 0.8$.

leaving the other parameters as in Fig. 2. Over short intervals we then merely observe the coherent $2T$ -periodic population exchange, as depicted in Fig. 3(a), while the expected Trojan beating manifests itself if we plot the population difference stroboscopically at multiples of $2T$ only, but for much longer durations, as done in Fig. 3(c). Here the observed Trojan tunneling time $T_0^{(\text{tun})}$, i.e., the duration of half a beating cycle, is $3865T$. For comparison, the Mathieu estimate (A32) derived in the Appendix gives $T_0^{(\text{tun})} \approx 1.9 \times 10^3 T$ and thus already provides the correct order of magnitude. We stress that the beating effect found here should not be attributed to the tunneling of individual Bose particles in the physical double-well potential constituting the Josephson junction, but rather to the tunneling of a single quasiparticle in the effective double cosine well in Fourier space. Quite similar observations are also made for significantly stronger driving: The tunneling signatures recorded in Figs. 3(b) and 3(d) emerge for $2\mu_1/\omega = 1.0$.

Within a mean-field ansatz, involving the introduction of a macroscopic wave function and the uncontrolled factorization of expectation values of operator products into products of expectation values [25], the dynamics of N Bose particles in the driven Josephson junction (12) are reduced to those of merely two amplitudes describing the population of the two wells. In terms of the population difference z and the relative phase ϕ which adopt the roles of momentum and its conjugate position coordinate, respectively, the mean-field dynamics coincides exactly with those of the driven, nonrigid classical pendulum governed by the Hamiltonian function [26,27]

$$H_{\text{mf}}(z, \phi, t) = N\kappa z^2 - \Omega\sqrt{1-z^2}\cos(\phi) + 2z(\mu_0 + \mu_1 \sin(\omega t)). \quad (14)$$

In Fig. 4 we show Poincaré sections for this classical nonlinear pendulum [20], obtained by recording typical trajectories T -stroboscopically in the ϕ - z plane. For the parameters chosen in Figs. 3(a) and 3(c) for illustrating Trojan tunneling, the 2:1 resonance manifests itself as two banana-shaped zones surrounding the central elliptic fixed point within a practically regular phase space, whereas the resonant islands are separated by a chaotic sea for the strong-driving scenario considered in

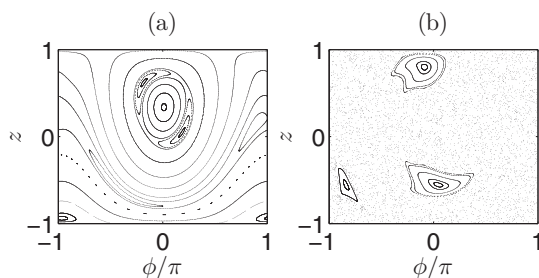


FIG. 4. Poincaré surfaces of section generated by the classical driven pendulum (14). (a) For the parameters underlying Figs. 3(a) and 3(c), the 2:1 resonance leads to two banana-shaped zones surrounding the central elliptic fixed point. (b) For the parameters of Figs. 3(b) and 3(d), the two resonant islands are separated by a chaotic sea; an additional regular island is visible in the lower left corner.

Figs. 3(b) and 3(d). In both cases the Trojan states $k = 0$ are semiclassically associated with the innermost “quantized” closed contours γ_k encircling the resonant stable $2T$ -periodic orbits which are selected by the Einstein-Brillouin-Keller conditions [8]

$$\frac{1}{2\pi} \oint_{\gamma_k} z d\phi = \frac{2}{N} \left(k + \frac{1}{2} \right); \quad (15)$$

observe that $2/N = \hbar_{\text{eff}}$ here plays the role of an effective Planck constant. In the classical case, as corresponding to the mean-field approximation to the full N -particle dynamics, a trajectory starting in one of the two equivalent resonant islands inevitably ends up in the other one after one period T , and returns to the first island after $2T$. The quasiparticle tunneling discussed in this work is a beyond-mean-field effect which can be regarded as a form of dynamical tunneling between symmetry-related regular regions of phase space [12,13]: After the Trojan tunneling time $T_0^{(\text{tun})}$ the N -particle state is semiclassically associated with the “wrong” island.

IV. DISCUSSION

Since single-particle Trojan states with $\nu = 1$ could be observed over about 15 000 cycles in microwave-driven Rydberg atoms [4], it seems feasible to detect Trojan beating for $\nu \geq 2$ with highly excited atoms in suitably tuned microwave fields. This already would constitute a spectacular demonstration of a genuine quantum effect. The search for Trojan many-body beating in driven bosonic Josephson junctions might break even further ground. Experimentally, one could generate Trojans in a robust manner by means of adiabatic switching [8], starting from the ground state. Because the population imbalance is a well-accessible observable, Trojan states with $\nu = 2$ can be identified through their subharmonic motion. The signature of Trojan quasiparticle tunneling then would be striking: After the tunneling time, the sloshing condensate is out of phase with the drive, being found in the “wrong” well. Since the Trojan quasiparticles (13), or those with even higher ν , correspond to highly entangled states, measurements of Trojan beating for different particle numbers could enable one to gain valuable information on the persistence (or nonpersistence) of entanglement with increasing N after long driving times.

This many-body aspect distinguishes our proposal from related recent works which have addressed dynamical tunneling with Bose-Einstein condensates in magnetic microtraps [28], or in a kicked-rotor experiment [29]: In such configurations one probes essentially single-particle physics, so that the effective Planck constant is determined by the parameters of the respective setup [28,29]. In contrast, Eq. (15) has shown that $\hbar_{\text{eff}} = 2/N$ in our case, so that here the “degree of quantumness” can be tuned by varying the particle number. This might be of interest for exploring quasiparticle tunneling in quasiregular situations exemplified by Fig. 4(a), or in chaotic situations as corresponding to Fig. 4(b), and for testing modern concepts of chaos-assisted tunneling [30] within a many-body setting.

The experimental exploitation of Trojan quasiparticles presupposes that the periodically driven Bose-Einstein condensate system possesses a well-preserved order parameter, in order

to render the existence of Floquet condensates possible. This requirement puts an upper limit on the sizes of the systems one could work with, since Floquet condensates tend to become unstable upon increasing N [8,31]. It is an open question whether one could detect signs of the onset of this instability in Trojan quasiparticle tunneling.

ACKNOWLEDGMENTS

We acknowledge support from the Deutsche Forschungsgemeinschaft (DFG) through Grant No. HO 1771/6-2. The computations were performed on the HPC cluster HERO, located at the University of Oldenburg and funded by the DFG through its Major Research Instrumentation Programme (INST 184/108-1 FUGG), and by the Ministry of Science and Culture (MWK) of the Lower Saxony State.

APPENDIX: MATHIEU ANALYSIS OF BEATING TROJANS

The starting point is the approximate system (6): Because each coefficient c_n is coupled to $c_{n\pm\nu}$ only, there are ν separate ‘‘ladders’’ of states (see Fig. 1 for $\nu = 2$) which we label by $j = 0, 1, \dots, \nu - 1$. Accordingly, we relabel the coefficients such that

$$c_{r+j+\ell\nu} \equiv b_\ell^{(j)}, \quad (\text{A1})$$

so that the index ℓ enumerates the members of the particular subset of coefficients specified by j . Since this implies

$$(n - r)^2 = \nu^2(\ell + j/\nu)^2, \quad (\text{A2})$$

we have ν uncoupled systems

$$i\hbar b_\ell^{(j)} = \frac{1}{2}\nu^2 E_r'' \left(\ell + \frac{j}{\nu} \right)^2 b_\ell^{(j)} + \frac{\lambda\nu}{2} \left(b_{\ell+1}^{(j)} + b_{\ell-1}^{(j)} \right). \quad (\text{A3})$$

Let us first reconsider the standard case $\nu = 1$ [14,15], meaning that there is only one ladder, $j = 0$. Then the above Eq. (A3) is a Fourier representation of the well-known Mathieu equation [32], which plays a central role in both the stability analysis of the Paul trap [1] and, closely related, in the analysis of the original Trojan wave packets [3]: Setting

$$b_\ell^{(0)}(t) = e^{-i\eta t/\hbar} \frac{1}{2\pi} \int_0^{2\pi} d\vartheta f(\vartheta) e^{-i\ell\vartheta}, \quad (\text{A4})$$

we immediately have

$$i\hbar b_\ell^{(0)} = \eta b_\ell^{(0)} \quad (\text{A5})$$

and

$$b_{\ell+1}^{(0)} + b_{\ell-1}^{(0)} = e^{-i\eta t/\hbar} \frac{1}{2\pi} \int_0^{2\pi} d\vartheta f(\vartheta) e^{-i\ell\vartheta} 2 \cos \vartheta. \quad (\text{A6})$$

Moreover,

$$\begin{aligned} \ell^2 b_\ell^{(0)} &= e^{-i\eta t/\hbar} \frac{1}{2\pi} \int_0^{2\pi} d\vartheta f(\vartheta) \left(-\frac{d^2}{d\vartheta^2} \right) e^{-i\ell\vartheta} \\ &= e^{-i\eta t/\hbar} \frac{1}{2\pi} \int_0^{2\pi} d\vartheta [-f''(\vartheta)] e^{-i\ell\vartheta}, \end{aligned} \quad (\text{A7})$$

provided that $f(\vartheta) = f(\vartheta + 2\pi)$, so that the partial integrations carried out here do not produce boundary terms. Thus,

for $\nu = 1$ Eq. (A3) transforms into

$$\eta f(\vartheta) = -\frac{1}{2} E_r'' f''(\vartheta) + \lambda\nu \cos \vartheta f(\vartheta), \quad (\text{A8})$$

which is a Mathieu equation; substituting $\vartheta = 2z$ and writing $f(2z) \equiv \chi(z)$ produces its standard form [32]

$$\left[\frac{d^2}{dz^2} + \alpha - 2q \cos(2z) \right] \chi(z) = 0 \quad (\text{A9})$$

with parameters

$$\alpha = \frac{8\eta}{E_r''}, \quad (\text{A10})$$

$$q = \frac{4\lambda\nu}{E_r''}. \quad (\text{A11})$$

Because of the periodic boundary condition $f(\vartheta) = f(\vartheta + 2\pi)$ imposed on f in order to guarantee the validity of Eq. (A7) we require π -periodic Mathieu functions $\chi(z) = \chi(z + \pi)$, which exist only if the parameter α adopts, for given q , one of the so-called characteristic values. Employing the widely accepted symbols a_n (giving even Mathieu functions) and b_n (giving odd ones) as defined in Ref. [32] for these quantities, the allowed values of α are

$$\alpha_k = \begin{cases} a_k, & k = 0, 2, 4, \dots \\ b_{k+1}, & k = 1, 3, 5, \dots \end{cases} \quad (\text{A12})$$

thus introducing a new quantum number k . This specifies the desired coefficients (A4) as

$$b_\ell^{(0)}(t) = e^{-i\eta_k t/\hbar} f_{\ell,k}, \quad (\text{A13})$$

writing

$$\eta_k = \frac{1}{8} \alpha_k E_r'' \quad (\text{A14})$$

in accordance with Eq. (A10), and denoting by $f_{\ell,k}$ the ℓ th Fourier coefficient of the Mathieu function associated with α_k . In this way we have found approximate solutions to the time-dependent Schrödinger equation of the driven nonlinear oscillator which conform to the ansatz (3) made in Sec. II:

$$|\Psi_k(t)\rangle = e^{-i\eta_k t/\hbar} \sum_\ell f_{\ell,k} |r + \ell\rangle \exp \left[-\frac{i}{\hbar} (E_r + \ell\hbar\omega) t \right]. \quad (\text{A15})$$

Obviously these solutions are Floquet states with quasienergies

$$\varepsilon_k = E_r + \eta_k \pmod{\hbar\omega}; \quad (\text{A16})$$

the ‘‘ground state’’ with $k = 0$ then corresponds to the non-spreading Trojan wave packet most strongly localized around the classical periodic orbit which is locked to the periodic drive in a 1:1 resonance [15].

The task now is to generalize this procedure, which so far applies to $\nu = 1$ only, to the case $\nu \geq 2$ which is a precondition for Trojan tunneling. If we started again from a representation (A4) for $b_\ell^{(j)}(t)$, with $f(\vartheta)$ appropriately replaced by $f^{(j)}(\vartheta)$, the analogs of Eqs. (A5) and (A6) would go through unchanged, but Eq. (A7) is of no use when $j \neq 0$. Instead, with a view towards Eq. (A3) we write

$$b_\ell^{(j)}(t) = e^{-i\eta t/\hbar} \frac{1}{\nu 2\pi} \int_0^{\nu 2\pi} d\vartheta g^{(j)}(\vartheta) e^{-i(\ell+j/\nu)\vartheta}, \quad (\text{A17})$$

where

$$g^{(j)}(\vartheta) = f^{(j)}(\vartheta) e^{i(j/v)\vartheta} \quad (\text{A18})$$

now obeys the crucial boundary condition

$$g^{(j)}(\vartheta) = g^{(j)}(\vartheta + v2\pi), \quad (\text{A19})$$

which is required for establishing the identity

$$\left(\ell + \frac{j}{v}\right)^2 b_\ell^{(j)} = e^{-i\eta t/\hbar} \frac{1}{v2\pi} \int_0^{v2\pi} d\vartheta \times [-g^{(j)''}(\vartheta)] e^{-i(\ell+j/v)\vartheta}. \quad (\text{A20})$$

This then leads to the Mathieu equation

$$\eta g^{(j)}(\vartheta) = -\frac{v^2}{2} E_r'' g^{(j)''}(\vartheta) + \lambda v \cos \vartheta g^{(j)}(\vartheta), \quad (\text{A21})$$

which again can be brought into the standard form (A9) by setting $g^{(j)}(2z) \equiv \chi(z)$, implying

$$\alpha = \frac{8\eta}{v^2 E_r''}, \quad (\text{A22})$$

$$q = \frac{4\lambda v}{v^2 E_r''}. \quad (\text{A23})$$

The key point now is the boundary condition (A19), which forces us to select $v\pi$ -periodic Mathieu functions $\chi(z) = \chi(z + v\pi)$. Because Eq. (A21) can be interpreted as the stationary Schrödinger equation for a quantum particle moving on a one-dimensional cosine lattice, the associated desired solutions (A18) then correspond to Bloch waves of this lattice, with periodic Born–von Kármán boundary conditions imposed after v potential wells [16]. We denote the discrete Bloch band index labeling these solutions by $k = 0, 1, 2, \dots$, in accordance with the notation employed in Eq. (A12) for $v = 1$. Thus, for each k we find the v different approximate solutions to the time-dependent Schrödinger equation of the driven nonlinear oscillator which have been heralded by Eq. (7), each one corresponding to a “ladder” of the type depicted in Fig. 1:

$$|\Psi_k^{(j)}(t)\rangle = e^{-i\eta_k^{(j)}t/\hbar} \sum_\ell f_{\ell,k}^{(j)} |r + j + \ell v\rangle \times \exp\left[-\frac{i}{\hbar}(E_r + j\hbar\omega/v + \ell\hbar\omega)t\right]. \quad (\text{A24})$$

Once again these solutions are Floquet states, now with quasienergies

$$\varepsilon_k^{(j)} = E_r + j\hbar\omega/v + \eta_k^{(j)} \pmod{\hbar\omega}. \quad (\text{A25})$$

In classical mechanics a $v:1$ resonance gives rise to v equivalent stable $v \times 2\pi/\omega$ -periodic orbits [20]. The above $2\pi/\omega$ -periodic Floquet states, corresponding to extended Bloch waves in a lattice with v wells, yield wave packets localized around *each* of these orbits, the sharpest localization being obtained for $k = 0$. In order to construct wave packets which follow *only one* orbit in a Trojan fashion, one has to take those linear combinations of the Bloch waves which produce a Wannier-like state localized in an individual well [16]. In contrast to single Floquet states such linear combinations are not stationary states, which is the reason for Trojan beating.

All essentials are made visible already by the case $v = 2$, which leads to a lattice with periodic boundary conditions imposed after two wells: Then one encounters the tunneling effect of a quasiparticle in a symmetric double-well potential, involving the superpositions

$$|\tilde{\Psi}_k^{(\pm)}\rangle = \frac{1}{\sqrt{2}}(|\Psi_k^{(0)}(t=0)\rangle \pm |\Psi_k^{(1)}(t=0)\rangle), \quad (\text{A26})$$

which correspond to states initially localized in the “left” or “right” well, respectively. Here the “ground-state doublet” $k = 0$ yields two strongly localized wave packets, each following closely, on short time scales, one of the two stable periodic orbits associated with the 2:1 resonance. While the quasienergies for $j = 0$ take the form

$$\varepsilon_k^{(0)} = E_r + \frac{1}{2}\alpha_k^{(0)} E_r'' \pmod{\hbar\omega}, \quad (\text{A27})$$

with $\alpha_k^{(0)}$ being given by Eq. (A12), one obtains

$$\varepsilon_k^{(1)} = E_r + \frac{1}{2}\hbar\omega + \frac{1}{2}\alpha_k^{(1)} E_r'' \pmod{\hbar\omega} \quad (\text{A28})$$

for $j = 1$, now requiring the Mathieu characteristic values associated with 2π -periodic Mathieu functions $\chi(z)$ [32]:

$$\alpha_k^{(1)} = \begin{cases} b_{k+1}, & k = 0, 2, 4, \dots \\ a_k, & k = 1, 3, 5, \dots \end{cases} \quad (\text{A29})$$

Evidently, the Trojan tunneling time—the time to evolve from $|\tilde{\Psi}_k^{(+)}\rangle$ to $|\tilde{\Psi}_k^{(-)}\rangle$, or to tunnel from one of the two $4\pi/\omega$ -periodic orbits to the other—is given by

$$T_k^{(\text{tun})} = \frac{2\pi\hbar}{E_r''(b_{k+1} - a_k)}, \quad (\text{A30})$$

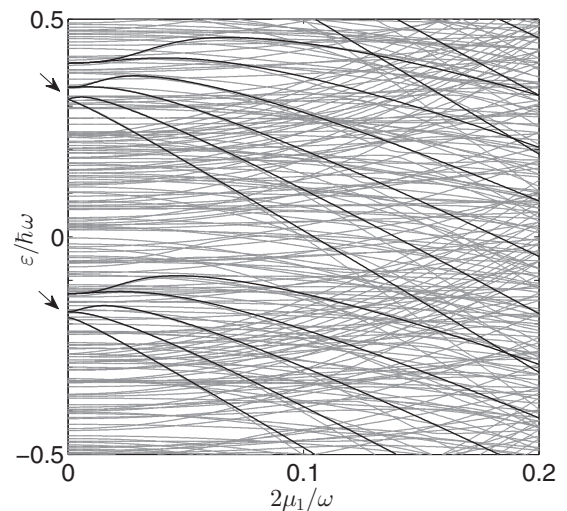


FIG. 5. Grey lines: Exact quasienergy spectrum of the tilted, driven bosonic Josephson junction for $N = 200$ particles, as also shown in Fig. 2 ($N\kappa/\Omega = 0.95$, $\omega/\Omega = 3.258$, $\mu_0/\Omega = 0.5$). Black lines: Quasienergies provided for $v = 2$ by the Mathieu approximations (A27) and (A28), with $r = 142$. The Mathieu parameter (A33) is given by $q\omega/(2\mu_1) = -498.26$.

which can be evaluated for large q by employing the asymptotic expression [32,33]

$$b_{k+1} - a_k \sim \frac{2^{4k+5}}{k!} \sqrt{\frac{2}{\pi}} q^{k/2+3/4} e^{-4\sqrt{q}}. \quad (\text{A31})$$

In particular, for the archetypal Trojan doublet with $k = 0$ one obtains the estimate

$$T_0^{(\text{tun})} \sim \frac{\pi^{3/2} \hbar}{16\sqrt{2} E_r''} q^{-3/4} e^{4\sqrt{q}}. \quad (\text{A32})$$

As is evident from the standard form (A9), the Mathieu parameter q determines the depth of the cosine lattice. In the case of the resonantly driven bosonic Josephson junction

defined by Eqs. (11) and (12) in Sec. III, it is calculated from

$$q = \frac{2}{v^2 E_r'' / (\hbar\omega)} \frac{2\mu_1}{\omega} \langle r | a_1^\dagger a_1 - a_2^\dagger a_2 | r - v \rangle. \quad (\text{A33})$$

Figure 5 provides a comparison of the exact quasienergies for the 2:1 resonance already considered in Fig. 2 to the corresponding approximations (A27) and (A28) provided by the Mathieu analysis. In view of the substantial simplifications which have led to its starting point (A3), the agreement is quite satisfactory, confirming that the essential features have been kept.

[1] W. Paul, *Rev. Mod. Phys.* **62**, 531 (1990).
 [2] I. Bialynicki-Birula, M. Kalański, and J. H. Eberly, *Phys. Rev. Lett.* **73**, 1777 (1994).
 [3] M. Kalinski and J. H. Eberly, *Phys. Rev. A* **53**, 1715 (1996).
 [4] H. Maeda and T. F. Gallagher, *Phys. Rev. Lett.* **92**, 133004 (2004).
 [5] B. Wyker, S. Ye, F. B. Dunning, S. Yoshida, C. O. Reinhold, and J. Burgdörfer, *Phys. Rev. Lett.* **108**, 043001 (2012).
 [6] J. Henkel and M. Holthaus, *Phys. Rev. A* **45**, 1978 (1992).
 [7] A. Buchleitner, D. Delande, and J. Zakrzewski, *Phys. Rep.* **368**, 409 (2002).
 [8] B. Gertjerenken and M. Holthaus, *New J. Phys.* **16**, 093009 (2014).
 [9] M. Albiez, R. Gati, J. Fölling, S. Hunsmann, M. Cristiani, and M. K. Oberthaler, *Phys. Rev. Lett.* **95**, 010402 (2005).
 [10] R. Gati and M. K. Oberthaler, *J. Phys. B* **40**, R61 (2007).
 [11] T. Zibold, E. Nicklas, C. Gross, and M. K. Oberthaler, *Phys. Rev. Lett.* **105**, 204101 (2010).
 [12] M. J. Davis and E. J. Heller, *J. Chem. Phys.* **75**, 246 (1981).
 [13] *Dynamical Tunneling: Theory and Experiment*, edited by S. Keshavamurthy and P. Schlagheck (CRC Press, Boca Raton, FL, 2011).
 [14] G. P. Berman and G. M. Zaslavsky, *Phys. Lett. A* **61**, 295 (1977).
 [15] M. Holthaus, *Chaos Solitons Fractals* **5**, 1143 (1995).
 [16] N. W. Ashcroft and N. D. Mermin, *Solid State Physics* (Harcourt, Fort Worth, TX, 1976).
 [17] J. H. Shirley, *Phys. Rev.* **138**, B979 (1965).
 [18] Ya. B. Zel'dovich, *Zh. Eksp. Teor. Fiz.* **51**, 1492 (1966) [*Sov. Phys. JETP* **24**, 1006 (1967)].
 [19] H. Sambe, *Phys. Rev. A* **7**, 2203 (1973).
 [20] J. V. José and E. J. Saletan, *Classical Dynamics: A Contemporary Approach* (Cambridge University Press, Cambridge, UK, 1998).
 [21] H. J. Lipkin, N. Meshkov, and A. J. Glick, *Nucl. Phys.* **62**, 188 (1965).
 [22] G. J. Milburn, J. Corney, E. M. Wright, and D. F. Walls, *Phys. Rev. A* **55**, 4318 (1997).
 [23] A. S. Parkins and D. F. Walls, *Phys. Rep.* **303**, 1 (1998).
 [24] A. Eckardt, T. Jinasundera, C. Weiss, and M. Holthaus, *Phys. Rev. Lett.* **95**, 200401 (2005).
 [25] A. J. Leggett, *Rev. Mod. Phys.* **73**, 307 (2001).
 [26] A. Smerzi, S. Fantoni, S. Giovanazzi, and S. R. Shenoy, *Phys. Rev. Lett.* **79**, 4950 (1997).
 [27] C. Weiss and N. Teichmann, *Phys. Rev. Lett.* **100**, 140408 (2008).
 [28] M. Lenz, S. Wüster, C. J. Vale, N. R. Heckenberg, H. Rubinsztein-Dunlop, C. A. Holmes, G. J. Milburn, and M. J. Davis, *Phys. Rev. A* **88**, 013635 (2013).
 [29] R. K. Shrestha, J. Ni, W. K. Lam, G. S. Summy, and S. Wimberger, *Phys. Rev. E* **88**, 034901 (2013).
 [30] S. Löck, A. Bäcker, R. Ketzmerick, and P. Schlagheck, *Phys. Rev. Lett.* **104**, 114101 (2010).
 [31] B. Gertjerenken and M. Holthaus, *Phys. Rev. A* **90**, 053614 (2014).
 [32] *Handbook of Mathematical Functions*, edited by M. Abramowitz and I. A. Stegun (Dover, New York, 1972).
 [33] J. Meixner and F. W. Schäfke, *Mathieusche Funktionen und Sphäroidfunktionen* (Springer-Verlag, Berlin, 1954).